Organometallics **2006,** *25,* 5817−5823

[1]Ferrocenophanes, [1]Chromarenophanes, and [1]Vanadarenophanes with Aluminium and Gallium in Bridging Positions

Clinton L. Lund,[‡] Jörg A. Schachner,[‡] J. Wilson Quail,[§] and Jens Müller[*,‡]

Department of Chemistry and Saskatchewan Structural Sciences Centre, University of Saskatchewan,
110 Science Place, Saskatoon, Saskatchewan S7N 5C9, Canada

Received August 14, 2006

Aluminum- and gallium-bridged [1]ferrocenophanes (**4a**, **4b**), [1]chromarenophanes (**5a**, **5b**), and [1]vanadarenophanes (**6a**, **6b**) were synthesized from the respective dilithiated sandwich compounds with element dichlorides $(Me_2Ntsi)ECl_2$ [E = Al, Ga; $Me_2Ntsi = C(SiMe_3)_2(SiMe_2NMe_2)$] in moderate to high isolated yields (54−97%). The new intramolecularly stabilized aluminum compound $(Me_2NCH_2\text{-}tsi)AlCl_2$ (**2a**) was synthesized, but was proven to be unreactive with respect to $[Fe(LiC_5H_4)_2]\cdot 2/3TMEDA$. The diamagnetic species **2a**, **4a**, **4b**, **5a**, and **5b** were characterized by NMR spectroscopy (^1H, ^{13}C, ^{27}Al), CHN elemental analysis, and mass spectrometry, whereas the paramagnetic compounds **6a** and **6b** were characterized by IR spectroscopy, CHN elemental analysis, and mass spectrometry. In addition, the molecular structures of compounds **2a**, **4a**, **4b**, **5a**, **5b**, **6a**, and **6b** were determined by single-crystal X-ray analysis. All [1]cyclophanes are strained species, as revealed by the following tilt angles α [deg]: 14.33(14) (**4a**), 15.83(19) (**4b**), 11.81(9) (**5a**), 13.24(13) (**5b**), 14.65(14) (**6a**), and 15.63(14) (**6b**).

Introduction

Since their discovery in 1975 by Osborne and Whiteley,[1] strained [1]ferrocenophanes containing main-group elements in the bridging position have sparked a lot of interest throughout the scientific community. Manners et al. showed that [1]ferrocenophanes ([1]FCPs) produce high molecular weight polyferrocenes via ring-opening polymerization (ROP).[2] Because of the incorporation of metals into the backbone of the polymer chain, these materials show interesting new properties (e.g., redox, magnetic, electrical, and chemical).[3−5] Over the last two decades, new [1]ferrocenophanes with bridging elements ranging from group 13 to 16 were synthesized and their use for polymer synthesis was explored.[6] However, group 13 [1]ferrocenophane chemistry was restricted to boron.[7−9]

Recently, by reactions of intramolecularly coordinated element dichlorides $(Pytsi)ECl_2$ [E = Al, Ga; $Pytsi = C(SiMe_3)_2SiMe_2(2\text{-}C_5H_4N)$] with dilithioferrocene, we isolated the first alumina[1]ferrocenophane (Al[1]FCP)[10] and the first galla[1]ferrocenophane (Ga[1]FCP)[11] (Figure 1).

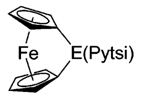

E = Al (**1a**), Ga (**1b**)

Figure 1. Al- and Ga[1]FCP [$Pytsi = C(SiMe_3)_2SiMe_2(2\text{-}C_5H_4N)$].

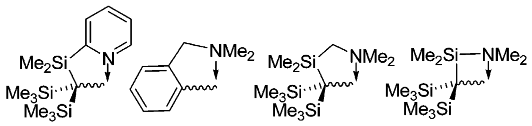

Pytsi **Ar'** **Me$_2$NCH$_2$tsi** **Me$_2$Ntsi**

Figure 2. Intramolecularly coordinating ligands.

The Pytsi ligand, derived from the well-known trisyl ligand $C(SiMe_3)_3$ by a formal substitution of one methyl group with a pyridyl ring, provides intramolecular coordination via the pyridyl moiety and steric shielding through the trimethylsilyl groups (Figure 2).[12]

In order to use strained [1]FCP as monomers for ROP, ideally, they should be accessible in high yields and high purities. In light of these requirements, the preparations of the Al[1]FCP **1a** and the Ga[1]FCP **1b** were unsatisfactory (Figure 1); yields were low to moderate and significant amounts of ferrocene were always produced during the synthesis. The aluminum compound **1a** (Figure 1) even crystallized with half of a molecule of $FeCp_2$ in the asymmetric unit.[10] Consequently, we focused our attention on improving the synthesis of Al- and Ga[1]FCPs by altering the ligand that remains attached at the bridging element. Furthermore, we started to explore the possibilities of using intramolecularly coordinated alanes and gallanes for the syn-

---

[*] Corresponding author. E-mail: jens.mueller@usask.ca.

[‡] Department of Chemistry.

[§] Saskatchewan Structural Sciences Centre.

(1) Osborne, A. G.; Whiteley, R. H. *J. Organomet. Chem.* **1975**, *101*, C27−C28.

(2) Foucher, D. A.; Tang, B. Z.; Manners, I. *J. Am. Chem. Soc.* **1992**, *114*, 6246−6248.

(3) Manners, I. *Chem. Commun.* **1999**, *10*, 857−944.

(4) Manners, I. *Science* **2001**, *294*, 1664−1666.

(5) Nguyen, P.; Gomez-Elipe, P.; Manners, I. *Chem. Rev.* **1999**, *99*, 1515−1548.

(6) Tanabe, M.; Vandermeulen, G. W. M.; Chan, W. Y.; Cyr, P. W.; Vanderark, L.; Rider, D. A.; Manners, I. *Nat. Mater.* **2006**, *5*, 467−470, and references therein.

(7) Berenbaum, A.; Braunschweig, H.; Dirk, R.; Englert, U.; Green, J. C.; Jäkle, F.; Lough, A. J.; Manners, I. *J. Am. Chem. Soc.* **2000**, *122*, 5765−5774.

(8) Braunschweig, H.; Dirk, R.; Müller, M.; Nguyen, P.; Resendes, R.; Gates, D. P.; Manners, I. *Angew. Chem., Int. Ed.* **1997**, *36*, 2338−2340.

(9) Braunschweig, H.; Breitling, F. M.; Gullo, E.; Kraft, M. *J. Organomet. Chem.* **2003**, *680*, 31−42.

(10) Schachner, J. A.; Lund, C. L.; Quail, J. W.; Müller, J. *Organometallics* **2005**, *24*, 785−787.

(11) Schachner, J. A.; Lund, C. L.; Quail, J. W.; Müller, J. *Organometallics* **2005**, *24*, 4483−4488.

(12) Eaborn, C.; Smith, J. D. *J. Chem. Soc., Dalton Trans.* **2001**, 1541−1552.

10.1021/om060736q CCC: $33.50

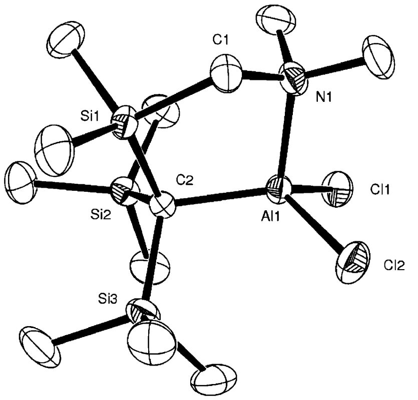

Figure 3. Molecular structure of **2a** with thermal ellipsoids at the 50% probability level. H atoms are omitted for clarity. Selected bond lengths [Å] and angles [deg]: Al1−N1 = 1.9783(12), Al1−C2 = 1.9805(13), Al1−Cl1 = 2.1501(5), Al1−Cl2 = 2.1661(5), N1−Al1−C2 = 103.80(5), N1−Al1−Cl1 = 106.42(4), N1−Al1−Cl2 = 100.24(4), C2−Al1−Cl1 = 119.03(4), C2−Al1−Cl2 = 117.37(4).

thesis of strained [1]metalloarenophanes. Our first results are described in this paper.

Results and Discussion

If the popular "one-armed phenyl" ligand (Ar′, Figure 2) is applied instead of the Pytsi ligand, [1.1]FCPs are produced exclusively (E = Al,[13,14] Ga,[14] In[14]). In our first attempt to improve the synthesis of an Al[1]FCP, we formally replaced the pyridyl donor of the Pytsi ligand by the saturated CH_2NMe_2 "arm" of the Ar′ ligand (Figure 2). By adapting known procedures, we synthesized the aluminum compound (Me_2NCH_2tsi)$AlCl_2$ (**2a**) (see Experimental Section for details). As expected, the molecular structure of compound **2a** reveals no surprises (Figure 3).

The Al atom in **2a** is coordinated similarly to that in the known compound (Pytsi)$AlCl_2$.[15] For both species, the central metal atom is surrounded by C, N, and two Cl atoms with bond lengths of 1.9783(12) Å (Al−N), 1.9805(13) Å (Al−C), 2.1501(5) Å (Al−Cl), and 2.1661(5) Å (Al−Cl) for compound **2a** (Figure 3) compared with 1.9383(16) Å (Al−N), 1.9784(19) Å (Al−C), 2.1295(8) Å (Al−Cl), and 2.1529(8) Å (Al−Cl) for (Pytsi)$AlCl_2$.[15] For both species, the set of four atoms around the Al atom form a similarly distorted tetrahedron. On the basis of this comparison, we expected a similar reactivity of **2a** relative to (Pytsi)$AlCl_2$. However, reaction of **2a** with dilithioferrocene, under conditions similar to those we applied for the syntheses of the [1]FCPs **1a** and **1b**,[10,11] revealed that the dichloride **2a** was significantly less reactive than (Pytsi)$AlCl_2$. ^{1}H NMR spectra taken from the reaction mixtures showed only small peaks in the typical range for Cp groups, indicating the presence of substituted ferrocenes; ca. 90% of the dichloride **2a** was still present in solution. None of the ^{1}H NMR signals indicated the presence of the targeted Al[1]FCP.

A drastic change in reactivity can be observed if, instead of Me_2NCH_2tsi ligand, the shorter Me_2Ntsi is employed (Figure 2). Alanes and gallanes of the type (Me_2Ntsi)ECl_2 were already

Scheme 1

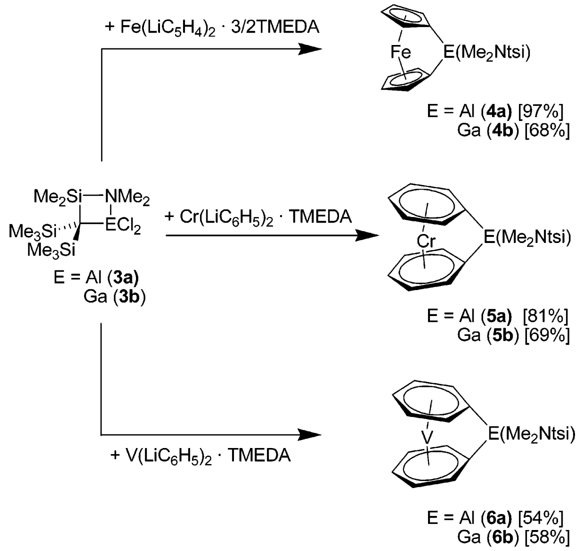

synthesized by Eaborn and Smith et al.[16] Reaction of (Me_2Ntsi)$AlCl_2$ (**3a**) with dilithioferrocene gave the new Al[1]FCP **4a** in an isolated yield of 97% (Scheme 1). Similarly, we synthesized the Ga[1]FCP **4b**. Encouraged by these results, we were able to synthesize the first aluminum- and gallium-bridged [1]chromarenophanes (**5a**,**b**) and the respective vanadium compounds (**6a**,**b**; Scheme 1).

[1]Ferrocenophanes. Compounds **4a** and **4b** both show signal patterns in the ^{1}H and ^{13}C NMR spectra that can be interpreted as being caused by [1]FCPs with time-averaged C_s symmetry. For example, the ^{1}H NMR spectrum of **4a** shows three pseudotriplets for the C_5H_4 rings with a 1:1:2 intensity ratio at δ 3.76 (α-H), 4.24 (α-H), and 4.58 (β-H). This signal pattern is similar to that of the Pytsi species **1a**,[10] except for the fact that the splitting of the β-protons in **4a** is so small that their signals overlap. The most indicative spectroscopic data to prove that indeed strained [1]FCPs were formed comes from ^{13}C NMR spectroscopy. The signal of the *ipso*-C atoms of the cyclopentadienyl ligands should be shifted upfield with respect to that of the $FeCp_2$ (δ 68). The detected shifts for **4a** (δ 53.0) and **4b** (δ 47.3) match very well with those of the [1]FCPs **1a** (δ = 52.9)[10] and **1b** (δ 47.2).[11]

The new [1]FCPs **4a** and **4b** are isomorphous and crystallized with half of a molecule of C_6H_6 in the asymmetric unit (Table 1); the molecular structure of the aluminum species **4a** is depicted in Figure 4 (ORTEP plot of **4b** see Supporting Information).

In both cases, the bridging element is part of a planar, four-membered ring [rms deviations from planarity [Å] are 0.0074 (**4a**), 0.0068 (**4b**)] and surrounded by one N atom and three C atoms. As expected, the E−C bonds are very similar for both species [Al1−C1 2.000(2), Al1−C6 1.988(2), Al1−C11 2.0301(19) Å for **4a**; Ga1−C1 2.008(3), Ga1−C6 2.017(3), Ga1−C11 2.048(3) Å for **4b**] and the E−N bonds are significantly different [Al1−N1 2.0123(17) and Ga1−N1 2.105(2) Å]. The extent of strain present in [1]FCPs can be expressed by a set of angles, among which the tilt angle α is the most common one (Figure 5).[17]

We determined tilt angles α of 14.33(14)° for **4a** and 15.83(19)° for **4b**. The value for **4a** is very close to that of 14.9(3)°

---

(13) Braunschweig, H.; Burschka, C.; Clentsmith, G. K. B.; Kupfer, T.; Radacki, K. *Inorg. Chem.* **2005**, *44*, 4906−4908.

(14) Schachner, J. A.; Orlowski, G. A.; Quail, J. W.; Kraatz, H.-B.; Müller, J. *Inorg. Chem.* **2006**, *45*, 454−459.

(15) Howson, J.; Eaborn, C.; Hitchcock, P. B.; Hill, M. S.; Smith, D. J. *J. Organomet. Chem.* **2005**, *690*, 69−75.

(16) Al-Juaid, S. S.; Eaborn, C.; El-Hamruni, S. M.; Hitchcock, P. B.; Smith, J. D. *Organometallics* **1999**, *18*, 45−52.

(17) See for example: Herberhold, M. *Angew. Chem., Int. Ed.* **1995**, *34*, 1837−1839.

Table 1. Crystal and Structural Refinement Data for Compounds 2a, 4a, and 4b

	2a	**4a**·1/2C_6H_6	**4b**·1/2C_6H_6
empirical formula	$C_{12}H_{32}AlCl_2NSi_3$	$C_{24}H_{41}AlFeNSi_3$	$C_{24}H_{41}FeGaNSi_3$
fw	372.54	510.68	553.42
wavelength, Å	0.71073	0.71073	0.71073
cryst syst	monoclinic	triclinic	triclinic
space group (no.)	$P2_1/c$ (14)	$P\bar{1}$ (2)	$P\bar{1}$ (2)
Z	4	2	2
a, Å	14.5558(2)	9.0703(2)	9.0689(3)
b, Å	10.5318(2)	9.1867(2)	9.1768(3)
c, Å	14.0477(2)	18.8627(3)	18.9466(6)
α, deg	90	79.4549(12)	79.2406(18
β, deg	101.3318(12)	85.2343(11)	85.294(2)
γ, deg	90	61.3777(10)	61.6414(16)
vol, $Å^3$	2111.51(6)	1356.36(5)	1363.14(8)
d(calc), mg/m^3	1.172	1.250	1.348
temp, K	173(2)	173(2)	173(2)
abs coeff, mm^{-1}	0.510	0.733	1.664
θ range, deg	2.43 to 30.04	2.56 to 30.51	2.69 to 27.60
no. of reflns collected	12 031	35 005	18 573
no. of indep reflns	6185 [R(int) = 0.0187]	8264 [R(int) = 0.0615]	6232 [R(int) = 0.0538]
abs corr	none	psi-scan	psi-scan
ref method	full-matrix least-squares on F^2		
no. of data/restr/params	6185/0/182	8264/0/281	6232/0/281
goodness-of-fit on F^2	1.024	1.025	1.040
final R indices [$I > 2\sigma(I)$]	R1 = 0.0340, wR2 = 0.0829	R1 = 0.0449, wR2 = 0.0942	R1 = 0.0403, wR2 = 0.0805
R indices (all data)	R1 = 0.0452, wR2 = 0.0886	R1 = 0.0739, wR2 = 0.1070	R1 = 0.0623, wR2 = 0.0900
largest diff peak and hole, e·$Å^{-3}$	0.340 and −0.353	0.333 and −0.534	0.371 and −0.541

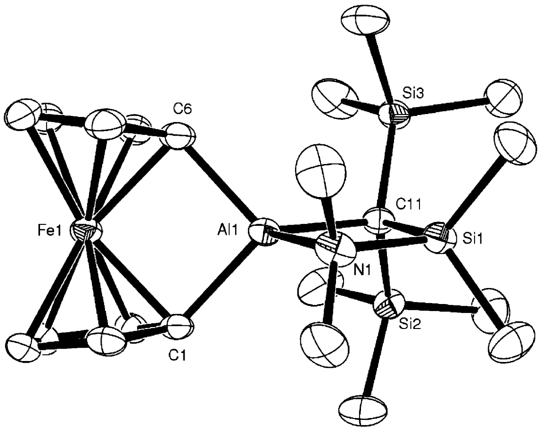

Figure 4. Molecular structure of **4a** with thermal ellipsoids at the 50% probability level. H atoms and 1/2 benzene are omitted for clarity. For an ORTEP plot of **4b** see Supporting Information. Selected atom−atom distances [Å] and bond angles [deg] for **4a**: Al1−N1 2.0123(17), Al1−C1 2.000(2), Al1−C6 1.988(2), Al1−C11 2.0301(19), Al1−Fe1 2.7708(6), C1−Al1−C6 94.51(8), N1−Al1−C11 86.71(7). Selected atom−atom distances [Å] and bond angles [deg] for **4b**: Ga1−N1 2.105(2), Ga1−C1 2.008(3), Ga1−C6 2.017(3), Ga1−C11 2.048(3), Ga1−Fe1 2.8184(5), C1−Ga1−C6 92.75(11), N1−Ga1−C11 84.98(10).

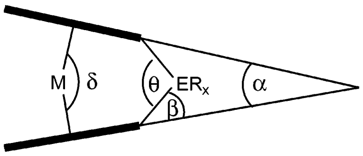

Figure 5. Set of angles to describe deformations in [1]metallocenophanes and [1]metalloarenophanes.

determined for the Pytsi-containing Al[1]FCP **1a** (Figure 1).[10] Compound **4b** is the first fully characterized Ga[1]FCP; the structural analysis of its Pytsi-containing counterpart **1b**[11] (Figure 1) did not allow the extraction of structural details like bond lengths and angles. The tilt angles α for **4a** and **4b** are similar as those determined for Sn[1]FCP [Sn*t*Bu_2 α = 14.1(2)°,[18] $SnMes_2$ α = 15.2(2)°[19]] and significantly smaller than those found for B[1]FCP, with the latter holding the record with 32.4(2)° for the largest known tilt angle in [1]FCP.[8] Even though the difference in the tilt of **4a** and **4b** is small, it is significant within three estimated standard deviations.

[1]Chromarenophanes and [1]Vanadarenophanes. Compared to [1]FCPs, only a few examples of [1]chromarenophanes ([1]CAPs) and [1]vanadarenophanes ([1]VAPs) are known in the literature. The first [1]CAPs and the first [1]VAPs were published in 1990 by Elschenbroich et al. ($SiPh_2$ moieties in bridging positions).[20] Since then, [1]CAPs have been described with silicon,[21−23] germanium,[24] zirconium,[25] and boron[26] in bridging positions.[27] Strained [1]VAPs are known with the bridging elements silicon,[20−22] germanium,[24] and zirconium.[25] Very recently, highly strained cyclophanes of cycloheptrienyl−cyclopentadienyl sandwich compounds, isoelectronic species to bis(benzene) complexes, have been characterized.[28−32]

We have synthesized the first aluminum- and gallium-bridged [1]chromarenophanes ([1]CAPs) and [1]vanadarenophanes ([1]-

---

[18] Rulkens, R.; Lough, A. J.; Manners, I. *Angew. Chem., Int. Ed.* **1996**, *35*, 1805−1807.

[19] Jäkle, F.; Rulkens, R.; Zech, G.; Foucher, D. A.; Lough, A. J.; Manners, I. *Chem. Eur. J.* **1998**, *4*, 2117−2128.

[20] Elschenbroich, C.; Hurley, J.; Metz, B.; Massa, W.; Baum, G. *Organometallics* **1990**, *9*, 889−897.

[21] Elschenbroich, C.; Bretschneider-Hurley, A.; Hurley, J.; Massa, W.; Wocadlo, S.; Pebler, J.; Reijerse, E. *Inorg. Chem.* **1993**, *32*, 5421−5424.

[22] Elschenbroich, C.; Bretschneider-Hurley, A.; Hurley, J.; Behrendt, A.; Massa, W.; Wocadlo, S.; Reijerse, E. *Inorg. Chem.* **1995**, *34*, 743−745.

[23] Hultzsch, K. C.; Nelson, J. M.; Lough, A. J.; Manners, I. *Organometallics* **1995**, *14*, 5496−5502.

[24] Elschenbroich, C.; Schmidt, E.; Gondrum, R.; Metz, B.; Burghaus, O.; Massa, W.; Wocadlo, S. *Organometallics* **1997**, *16*, 4589−4596.

[25] Elschenbroich, C.; Schmidt, E.; Metz, B.; Harms, K. *Organometallics* **1995**, *14*, 4043−4045.

[26] Braunschweig, H.; Homberger, M.; Hu, C. H.; Zheng, X. L.; Gullo, E.; Clentsmith, G.; Lutz, M. *Organometallics* **2004**, *23*, 1968−1970.

[27] For a historical overview and leading references about bis(benzene)-chromium chemistry see: Seyferth, D. *Organometallics* **2002**, *21*, 1520−1530.

[28] Elschenbroich, C.; Paganelli, F.; Nowotny, M.; Neumüller, B.; Burghaus, O. Z. *Anorg. Allg. Chem.* **2004**, *630*, 1599−1606.

Table 2. Crystal and Structural Refinement Data for Compounds 5a,b and 6a,b

	5a·1/2C_6H_6	**5b**·1/2C_6H_6	**6a**·1/2C_6H_6	**6b**·1/2C_6H_6
empirical formula	$C_{26}H_{43}AlCrNSi_3$	$C_{26}H_{43}CrGaNSi_3$	$C_{26}H_{43}AlNSi_3V$	$C_{26}H_{43}GaNSi_3V$
fw	532.86	575.60	531.80	574.54
wavelength, Å	0.71073	0.71073	0.71073	0.71073
cryst syst	triclinic	triclinic	triclinic	triclinic
space group (no.)	$P\bar{1}$ (2)	$P\bar{1}$ (2)	$P\bar{1}$ (2)	$P\bar{1}$ (2)
Z	2	2	2	2
a, Å	8.96730(10)	8.9883(2)	8.9681(3)	8.9868(3)
b, Å	9.16420(10)	9.1772(2)	9.1579(3)	9.1721(3)
c, Å	19.6077(3)	19.6458(4)	19.6320(5)	19.6692(5)
α, deg	81.9412(11)	81.3833(14)	82.0285(18)	81.577(2)
β, deg	89.5973(11)	89.3431(14)	89.204(2)	89.047(2)
γ, deg	63.0923(11)	63.0831(11)	63.2623(17)	63.324(2)
vol, $Å^3$	1419.78(3)	1425.74(6)	1423.90(8)	1430.88(8)
d(calc), mg/m^3	1.246	1.341	1.240	1.334
temp, K	173(2)	173(2)	173(2)	173(2)
abs coeff, mm^{-1}	0.575	1.467	0.520	1.408
θ range, deg	2.52 to 30.50	2.52 to 30.51	2.52 to 27.58	2.52 to 27.54
no. of reflns collected	36 806	39 640	20 973	21 117
no. of indep reflns	8649 [R(int) = 0.0563]	8694 [R(int) = 0.0741]	6521 [R(int) = 0.0766]	6560 [R(int) = 0.0602]
abs correction	psi-scan	psi-scan	psi-scan	psi-scan
ref method	full-matrix least-squares on F^2			
no. of data/restr/params	8649/0/299	8694/0/299	6521/0/299	6560/0/299
goodness-of-fit on F^2	1.026	1.036	1.027	1.034
final R indices [$I > 2\sigma(I)$]	R1 = 0.0425, wR2 = 0.0984	R1 = 0.0469, wR2 = 0.0932	R1 = 0.0510, wR2 = 0.1034	R1 = 0.0403, wR2 = 0.0820
R indices (all data)	R1 = 0.0608, wR2 = 0.1089	R1 = 0.0776, wR2 = 0.1067	R1 = 0.0874, wR2 = 0.1205	R1 = 0.0610, wR2 = 0.0918
largest diff peak and hole, e·$Å^{-3}$	0.384 and −0.609	0.564 and −0.722	0.333 and −0.455	0.362 and −0.537

VAPs) in isolated yields of 54−81% from slurries of dilithiated metalloarenes and the dihalogen species **3a** and **3b**, respectively (Scheme 1). Usually, we apply ^{1}H NMR spectroscopy to check on the progress of a new reaction. However, the vanadium compounds are paramagnetic and inaccessible for NMR spectroscopy, and consequently, we started with the syntheses of the chromium compounds. The optimized synthetic procedures for **5a** and **5b** were then adapted for the syntheses of the vanadium compounds **6a** and **6b**.

The [1]CAPs **5a** and **5b** show the expected signal pattern for time-averaged C_s symmetrical species in the ^{1}H and ^{13}C NMR spectra. For example, the aluminum compound **5a** exhibits five signals for the benzene rings [δ 3.74 and 4.35 (*o*-H), 4.53 and 4.60 (*m*-H), and 4.87 (*p*-H)], whereas in the case of the gallium counterpart **5b** a coincidental equivalency of the *meta* and *para* protons results in just three signals [δ 3.69 and 4.18 (*o*-H), 4.74 (*m*-H and *p*-H)]. All these proton signals are relatively broad, and their width depends on how often a particular compound had been manipulated. ^{1}H NMR spectra with the smallest peak width and best resolved structure of the aromatic protons were obtained from freshly synthesized samples. Elschenbroich et al. described a similar phenomenon for $[(Ph_3SiC_6H_5)_2Cr]$. It was proposed that the presence of the paramagnetic chromium(I) species $[(Ph_3SiC_6H_5)_2Cr]^+$ leads to a fast electron transfer with the neutral species $[(Ph_3SiC_6H_5)_2Cr]$, resulting in line broadening.[20] Electron exchange reactions of this type had been investigated before.[33] On the basis of these results, and in the absence of direct experimental evidence, we can only speculate that small amounts of the paramagnetic chromium(I) species **5a**$^+$ and **5b**$^+$, respectively, are responsible for the observed line broadening. The ^{13}C NMR spectra clearly reveal that both products **5a** and **5b** are strained [1]CAP. The resonances of the *ipso*-C atoms at δ 62.1 (**5a**) and 56.6 (**5b**) are significantly upfield shifted with respect to the parent bis(benzene)chromium (δ 74.8).[34] More pronounced upfield shifts are exhibited by the known [1]CAPs with $SiMe_2$ (δ 39.5),[23] $GeMe_2$ (δ 37.5),[24] $GePh_2$ (δ 36.4),[24] and $Zr(tBuC_5H_4)_2$ (δ 30.7).[25]

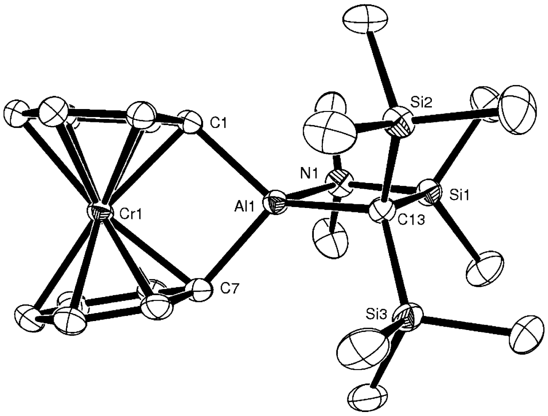

Figure 6. Molecular structure of **5a** with thermal ellipsoids drawn at the 50% probability level. H atoms and 1/2 benzene are omitted for clarity. For an ORTEP plot of **5b** see Supporting Information. Selected atom−atom distances [Å] and bond angles [deg] for **5a**: Al1−N1 = 2.0257(15), Al−C1 = 1.9979(17), Al1−C7 = 1.9940(17), Al1−C13 = 2.0412(16), Al1−Cr1 = 2.9740(5), C7−Al−C1 = 91.93(7), C7−Al1−N1 = 118.15(7), C1−Al1−N1 = 110.54(7), C7−Al1−C13 = 122.40(7), C1−Al−C13 = 129.30(7), N1−Al1−C13 = 86.47(6). Selected bond lengths (Å), atom−atom distances [Å], and angles [deg] for **5b**: Ga1−N1 = 2.121(2), Ga−C1 = 2.017(2), Ga1−C7 = 2.012(3), Ga1−C13 = 2.055(2), Ga1−Cr1 = 3.0256(5), C7−Ga−C1 = 89.77(10), C7−Ga1−N1 = 117.79(9), C1−Ga1−N1 = 109.85(9), C7−Ga1−C13 = 124.90(10), C1−Ga1−C13 = 131.70(10), N1−Ga1−C13 = 86.50(9).

---

(29) Tamm, M.; Kunst, A.; Bannenberg, T.; Herdtweck, E.; Sirsch, P.; Elsevier, C. J.; Ernsting, J. M. *Angew. Chem., Int. Ed.* **2004**, *41*, 5530−5534.

(30) Braunschweig, H.; Lutz, M.; Radacki, K. *Angew. Chem., Int. Ed.* **2005**, *44*, 5647−5651.

(31) Bartole-Scott, A.; Braunschweig, H.; Kupfer, T.; Lutz, M.; Manners, I.; Nguyen, T.-l.; Radacki, K.; Seeler, F. *Chem. Eur. J.* **2006**, *12*, 1266−1273.

(32) Braunschweig, H.; Lutz, M.; Radacki, K.; Schaumlöffel, A.; Seeler, F.; Unkelbach, C. *Organometallics* **2006**, *25*, 4433−4435.

(33) Elschenbroich, C.; Zenneck, U. *J. Organomet. Chem.* **1978**, *160*, 125−137.

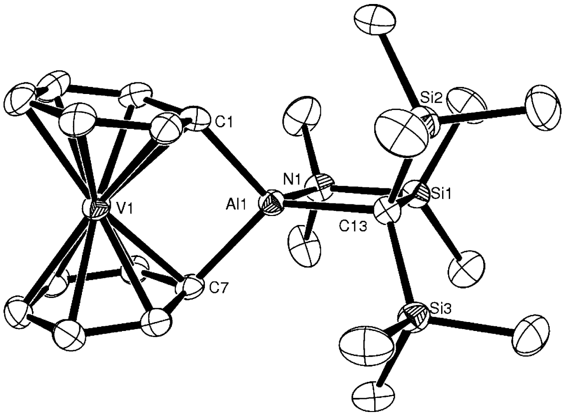

Figure 7. Molecular structure of **6a** with thermal ellipsoids drawn at the 50% probability level. H atoms and 1/2 benzene are omitted for clarity. For an ORTEP plot of **6b** see Supporting Information Selected atom−atom distances [Å] and bond angles [deg] for **6a**: Al1−N1 = 2.020(2), Al−C1 = 1.985(3), Al1−C7 = 1.995(3), Al1−C13 = 2.039(3), Al1−V1 = 2.9805(9), C7−Al−C1 = 93.78(11), C7−Al1−N1 = 110.27(11), C1−Al1−N1 = 117.52(11), C7−Al1−C13 = 128.51(11), C1−Al−C13 = 121.77(11), N1−Al1−C13 = 86.50(10). Selected atom−atom distances [Å] and bond angles [deg] for **6b**: Ga1−N1 = 2.122(2), Ga−C1 = 2.017(3), Ga1−C7 = 2.007(3), Ga1−C13 = 2.053(2), Ga1−V1 = 3.0212(5), C7−Ga−C1 = 92.37(10), C7−Ga1−N1 = 117.21(11), C1−Ga1−N1 = 109.29(10), C7−Ga1−C13 = 124.15(10), C1−Ga1−C13 = 130.34(11), N1−Ga1−C13 = 84.53(9).

Table 3. Deformation Angles α, *θ*, and *δ* [deg] of 5 and 6 (see Figure 5)

	5a [**5b**]	**6a** [**6b**]
α	11.81(9) [13.24(13)]	14.65(14) [15.63(14)]
θ	91.93(7) [89.77(10)]	93.78(11) [92.37(10)]
δ[a]	170.63(7) [169.43(11)]	168.43(11) [167.30(11)]

[a] It was assumed that the *δ* angles have esd's similar to those found for respective C−M−C angles (M = Cr, V; C: aromatic C atoms). The largest esd of C−M−C angles was taken for *δ*.

The [1]CAPs **5a** and **5b** and the [1]VAPs **6a** and **6b** all crystallized with half of a molecule of benzene in the asymmetric unit; all four compounds are isomorphous. Table 2 compiles crystal and structural refinement data, and Figures 6 and 7 depict molecular structures of the aluminum species (ORTEP plots of the gallium compounds **5b** and **6b** see Supporting Information).

As in the case of the [1]FCPs **4a** and **4b** described before, the [1]CAPs and [1]VAPs show planar heterocycles containing the bridging elements aluminum and gallium, respectively [rms deviations from planarity [Å] are 0.0082 (**5a**), 0.0042 (**5b**), 0.0050 (**6a**), 0.0042 (**6b**)]. The bridging elements are distorted tetrahedrally surrounded by three C and one N atom. Al−C distances are slightly shorter than respective Ga−C distances; respective E−C bond lengths are similar for the chromium and the vanadium species (Figures 6 and 7). Expectedly, E−N donor bonds are significantly shorter for aluminum than for gallium [Al1−N1 = 2.0257(15) (**5a**), Ga1−N1 = 2.121(2) (**5b**), Al1−N1 = 2.020(2) (**6a**), Ga1−N1 = 2.122(2) (**6b**)], which exemplifies that the lighter group 13 element is the stronger Lewis acid with respect to the NMe_2 donor group.

The alumina- and galla[1]metalloarenophanes **5** and **6** are strained species. Table 3 shows the set of common deformation angles α, *θ*, and *δ* (Figure 5) of the four species.

For the chromium and the vanadium compounds, respectively, the benzene rings are more tilted for the gallium-bridged species than for the aluminum-bridged species. The differences between the angles α for the [1]CAPs **5a** and **5b** of 1.4° and for the [1]VAPs **6a** and **6b** of 1.0° are small but significant. A similar trend was observed for the [1]FCPs **4a** and **4b** discussed before (1.5°). The α angles of known [1]CAPs are 14.4° ($SiPh_2$),[20] 16.6(3)° ($SiMe_2$),[23] 14.4(2)° ($GePh_2$),[24] and 26.6(3)° [BN*i*Pr($SiMe_3$)][26]; those of [1]VAPs are 20.8° [SiRR′],[21] 19.9° [Si(CH_2)$_3$],[22] and 8° [Zr(*t*BuC_5H_4)$_2$].[25]

Conclusion

Six new strained organometallic species were synthesized and structurally characterized. For all six species, the bridging Al and Ga atom, respectively, are equipped with the same trisyl-based ligand Me_2Ntsi (Figure 2). Hence, within the pairs of compounds **4a**,**b**, **5a**,**b**, and **6a**,**b**, respectively, only the bridging element differs, and this close relation allows revealing the influence of aluminum versus gallium as a bridging element. Commonly, the tilt angle α is taken as a measure of the extent of strain in cyclophanes (Figure 5). One major factor that governs α is the size of the bridging element. On the basis of covalent radii of 1.25 Å for aluminum and of 1.26 Å for gallium alone (singly bonded, 3-fold-coordinated elements),[35] a similar or a slightly higher tilt angle for the aluminum-bridged species **4a**, **5a**, and **6a** in comparison with the respective gallium-bridged species would be expected; surprisingly, just the opposite is the case. However, a glance at the neighboring group 14 elements Si and Ge reveals a similar situation, if only those molecules are compared that are equipped with the same set of ligands at the bridging element. On the basis of covalent radii of 1.17 Å for Si and of 1.22 Å for Ge alone (singly bonded tetracoordinated elements),[35] smaller angles of α are expected for germanium-bridged species. However, for [1]CAPs with $SiPh_2$ and $GePh_2$ in bridging positions, respectively, the same value of α was detected [14.4(2)°].[24] Similarly, for [1]FCPs with $SiMe_2$ [α = 20.8(5)°][36] and $GeMe_2$ [α = 19.0(9)°][37] bridging moieties, the tilt angles α are the same within three estimated standard deviations. Causes for these small structural differences are unknown today.

With the synthesis of the new strained molecules **4**−**6** on hand, we started to explore their chemistry, in particular with respect to polymerizations. Initial DSC measurements for **4a** and **4b**, respectively, showed exothermic peaks above 210 °C, a typical indication that ROP occurred.

Experimental Section

General Procedures. All manipulations were carried out using standard Schlenk techniques. Solvents were dried using a Braun solvent purification system and stored under nitrogen over 4 Å molecular sieves. All solvents for NMR spectroscopy were degassed prior to use and stored under nitrogen over 4 Å molecular sieves. [Fe(LiC_5H_4)$_2$]·2/3TMEDA,[38] [Cr(C_6H_6)$_2$],[39] [V(C_6H_6)$_2$],[40] $AlCl_2$-

---

(34) Elschenbroich, C.; Koch, J. *J. Organomet. Chem.* **1982**, *229*, 139−158.

(35) Holleman-Wiberg *Inorganic Chemistry*, 1st English ed.; Academic Press: San Diego, 2001; p 1756.

(36) Finckh, W.; Tang, B. Z.; Foucher, D. A.; Zamble, D. B.; Ziembinski, R.; Lough, A.; Manners, I. *Organometallics* **1993**, *12*, 823−829.

(37) Foucher, D. A.; Edwards, M.; Burrow, R. A.; Lough, A. J.; Manners, I. *Organometallics* **1994**, *13*, 4959−4966.

(38) Butler, I. R.; Cullen, W. R.; Ni, J.; Rettig, S. J. *Organometallics* **1985**, *4*, 2196−2201.

(39) *Synthetic Methods of Organometallic and Inorganic Chemistry*; Herrmann, W. A., Ed.; Georg Thieme Verlag Stuttgart: New York, 1997; Vol. 8.

(40) Fischer, E. O.; Reckziegel, A. *Chem. Ber.* **1961**, *94*, 2204−2208.

[C(SiMe$_3$)(SiMe$_2$NMe$_2$)] (**3a**),[16] and GaCl$_2$[C(SiMe$_3$)(SiMe$_2$NMe$_2$)] (**3b**)[16] were synthesized as described in the literature. ^{1}H, ^{13}C, and ^{27}Al NMR spectra were recorded on a Bruker 500 MHz Avance at 25 °C, unless noted differently. ^{1}H chemical shifts were referenced to the residual protons of the deuterated solvents (C$_6$D$_6$ at δ 7.15); ^{13}C chemical shifts were referenced to the C$_6$D$_6$ signal at δ 128.0; ^{27}Al NMR spectra were referenced to [Al(acac)$_3$] dissolved in C$_6$D$_6$. Mass spectra were measured on a VG 70SE (m/z > 10% are listed for signals of the most abundant ions). Elemental analyses were performed on a Perkin-Elmer 2400 CHN elemental analyzer using V$_2$O$_5$ to promote complete combustion.

HC(SiMe$_3$)$_2$SiMe$_2$CH$_2$NMe$_2$ (Me$_2$NCH$_2$tsiH). HC(SiMe$_3$)$_2$Si(Me$_2$)Br[41] (3.697 g, 12.4 mmol) in diethyl ether (30 mL) was added to LiCH$_2$NMe$_2$[42] (0.800 g, 12.3 mmol) in diethyl ether (20 mL) at −78 °C. The dry ice bath was removed and the solution stirred for 1 h to give a yellow solution. Volatiles were removed in vacuum, and the product was extracted with hexane (3 × 10 mL). After removal of hexane in vacuum, a yellow oil of HC(SiMe$_3$)$_2$SiMe$_2$CH$_2$NMe$_2$ was left behind (3.41 g, 99%). ^{1}H NMR (500 MHz): δ −0.56 (s, 1H, CH), 0.17 (s, 18H, SiMe$_3$), 0.23 (s, 6H, SiMe$_2$), 1.83 (s, 2H, CH$_2$), 2.15 (s, 6H, NMe$_2$).

(Me$_2$NCH$_2$tsi)AlCl$_2$ (2a). Due to an unsuccessful usage of **2a** as a starting material for [1]FCPs, the following procedure was not optimized. MeLi (11.5 mL, 1.0 M in THF, 11.5 mmol) was added to HC(SiMe$_3$)$_2$SiMe$_2$CH$_2$NMe$_2$ (2.87 g, 10.4 mmol) in THF (15 mL) at ambient temperature. After stirring for 1 h all volatiles were removed in vacuum to give an orange solid. Diethyl ether (20 mL) was added and AlCl$_3$ (1.42 g, 10.6 mmol) in diethyl ether (30 mL) was added at −78 °C. The mixture was stirred for 16 h at ambient temperature and filtered, and the solids were washed with 20 mL of diethyl ether. The combined filtrates were concentrated to 20 mL, and crystallization at ca. −30 °C gave yellow cubes of **2a** (1.41 g, 36%). ^{1}H NMR (500 MHz): δ 0.10 (s, 6H, SiMe$_2$), 0.44 (s, 18H, SiMe$_3$), 1.48 (s, 2H, CH$_2$), 1.99 (s, 6H, NMe$_2$). ^{13}C NMR: δ 4.1 (SiMe$_2$), 5.8 (CSi$_3$), 7.4 (SiMe$_3$), 49.9 (NMe$_2$), 54.6 (CH$_2$). ^{27}Al NMR (130.3 MHz): δ 131 ($h_{1/2}$ = 800 Hz). MS (70 eV): m/z (%) 356 (100) [M$^+$ − Me], 244 (62) [C$_{10}$H$_{26}$NSi$_3$$^+$], 73 (50) [SiMe$_3$$^+$]. Anal. Calcd for C$_{12}H_{32}$AlCl$_2NSi_3$ (372.536): C, 38.69; H, 8.66; N, 3.76. Found: C, 38.45; H, 8.93; N, 3.11.

Al[1]FCP (4a). A suspension of dilithioferrocene·2/3TMEDA (0.874 g, 3.17 mmol)[38] in toluene (15 mL) was added dropwise via tubing to a solution of **3a** (1.04 g, 2.90 mmol)[16] in toluene (15 mL; −20 °C). After stirring for 16 h at ambient temperature, the red solution was filtered and all volatiles were removed at high vacuum (25 °C/0.01 mbar), upon which crystallization of pure **4a** occurred (1.33 g, 2.82 mmol, 97%). Single crystals of **4a**·1/2C$_6$H$_6$ for X-ray analysis were grown from benzene solutions at ca. 8 °C. ^{1}H NMR (500 MHz): δ 0.18 (s, 6H, SiMe$_2$), 0.45 (s, 18H, SiMe$_3$), 2.11 (s, 6H, NMe$_2$), 3.76, 4.24 (pst, 4H, C$_5$H$_4$), 4.58 (pst, 4H, C$_5$H$_4$). ^{13}C NMR (125.8 MHz): δ 2.9 (SiMe$_2$), 7.7 (SiMe$_3$), 40.9 (NMe$_2$), 53.0 (*ipso*-C, C$_5$H$_4$, −40 °C, C$_7$D$_8$), 75.4, 75.6, 75.9, 76.1 (C$_5$H$_4$); signal of *C*(SiMe$_3$)$_2$ not detected. ^{27}Al NMR (130.3 MHz): δ 154 ($h_{1/2}$ = 4300 Hz). MS (70 eV): m/z (%) 471 (100) [M$^+$], 456 (27) [M$^+$ − Me], 186 (12) [FeCp$_2$$^+$], 73 (10) [SiMe$_3$$^+$]. Anal. Calcd for C$_{21}H_{38}$AlFeNSi$_3$ (471.62): C, 53.48; H, 8.12; N, 2.97. Found: C, 53.65; H, 8.35; N, 2.70.

Ga[1]FCP (4b). As described for **4a**, dilithioferrocene·2/3TMEDA (1.17 g, 4.25 mmol)[38] in toluene (20 mL) and **3b** (1.70 g, 4.24 mmol)[16] in toluene (20 mL; −20 °C) resulted in a crude product of **4b**. Recrystallization from toluene yielded red, needle-shaped crystals of **4b** (1.48 g, 2.88 mmol, 68%). Single crystals of **4b**·1/2C$_6$H$_6$ for X-ray analysis were grown from benzene solutions at ca. 8 °C. ^{1}H NMR (500 MHz): δ 0.19 (s, 6H, SiMe$_2$), 0.42 (s, 18H, SiMe$_3$), 2.15 (s, 6H, NMe$_2$), 3.90, 4.24 (pst, 4H, C$_5$H$_4$), 4.54 (pst, 4H, C$_5$H$_4$). ^{13}C NMR (125.8 MHz): δ 3.0 (SiMe$_2$), 6.7 (SiMe$_3$), 41.9 (NMe$_2$), 47.2 (*ipso*-C, C$_5$H$_4$), 75.3, 76.2, 76.5 (C$_5$H$_4$); signal of *C*(SiMe$_3$)$_2$ not detected. MS (70 eV): m/z (%) 513 (10) [M$^+$], 186 (100) [FeCp$_2$$^+$], 121 (22) [FeCp$^+$], 73 (6) [SiMe$_3$$^+$], 58 (16) [Fe$^+$]. Anal. Calcd for C$_{21}H_{38}$GaFeNSi$_3$ (514.361): C, 49.04; H, 7.45; N, 2.72. Found: C, 49.93; H, 7.70; N, 2.42.

Al[1]CAP (5a). *n*BuLi (3.2 mL, 2.6 M in hexanes, 8.3 mmol) was added dropwise to a refluxing solution of [Cr(C$_6$H$_6$)$_2$] (0.638 g, 3.06 mmol) and TMEDA (1.217 g, 10.47 mmol) in cyclohexane (30 mL).[20] After refluxing for 1 h, the red reaction mixture was cooled to 0 °C, the liquid phase was removed via syringe, and the residual solid was dried on high vacuum (0.646 g, 1.92 mmol). A slurry of this solid in diethyl ether (30 mL, −20 °C) was added to a solution of **3a** (0.690 g, 1.92 mmol) in diethyl ether (10 mL, −20 °C). The reaction mixture was stirred for 16 h at ambient temperature and filtered, and additional product was extracted with diethyl ether (2 × 10 mL) from the filter cake. From the combined organic phases, all volatiles were removed in vacuum, resulting in a crude solid, which was washed with hexane (3 × 15 mL) to give **5a** as a red-brown solid (0.490 g). Concentration of the washings to 10 mL gave an additional 0.272 g of **5a** (overall yield 0.762 g, 81%). Single crystals of **5a**·1/2C$_6$H$_6$ for X-ray analysis were grown from benzene solutions at ca. 8 °C. ^{1}H NMR (500 MHz, C$_6$D$_6$): δ 0.20 (s, 6H, SiMe$_2$), 0.49 (s, 18 H, 2 SiMe$_3$), 2.14 (s, 6H, NMe$_2$), 3.74 (d, 2H, *o*-H), 4.35 (d, 2H, *o*-H), 4.53 (pst, 2H, *m*-H), 4.60 (pst, 2H, *m*-H), 4.87 (pst, 2H, *p*-H). ^{13}C NMR: δ 3.0 (SiMe$_2$), 7.9 (2 SiMe$_3$), 9.2 (AlCSiMe$_3$) 40.6 (NMe$_2$), 62.1 (*ipso*-C), 77.6 (*p*-C), 77.9 (*o*-C), 78.4 (*o*-C), 80.7 (*m*-C), 81.2 (*m*-C). ^{27}Al NMR: δ 154 ($h_{1/2}$ = 3400 Hz). MS (70 eV): m/z (%) 493 (100) [C$_{23}$H$_{40}$CrAlNSi$_3$]$^+$, 450 (18) [C$_{21}$H$_{35}$AlCrSi$_3$]$^+$, 364 (95) [C$_{17}$H$_{35}$AlNSi$_3$]$^+$, 319 (16) [C$_{15}$H$_{28}$AlSi$_3$]$^+$, 287 (32) [C$_{11}$H$_{30}$AlNSi$_3$]$^+$, 247 (18), 230 (39) [C$_9$H$_{24}$NSi$_3$]$^+$, 201 (20) [C$_8$H$_{21}$Si$_3$]$^+$, 187 (18) [C$_7$H$_{19}$Si$_3$]$^+$, 175 (25), 129 (16) [C$_5$H$_{13}$Si$_2$]$^+$, 78 (32) [C$_6$H$_6$]$^+$, 73 (39) [C$_3$H$_9$Si]$^+$, 69 (49), 59 (13). Anal. Calcd for C$_{23}$H$_{40}$AlCrNSi$_3$ (493.810): C, 55.94; H, 8.16; N, 2.84. Found: C, 54.80; H, 8.58; N, 2.82.

Ga[1]CAP (5b). As described for **5a**, *n*BuLi (3.8 mL, 2.6 M in hexanes, 9.8 mmol), [Cr(C$_6$H$_6$)$_2$] (0.8112 g, 3.89 mmol), TMEDA (1.339 g, 8.64 mmol), and cyclohexane (25 mL)[20] resulted in a solid (0.923 g, 2.74 mmol). A slurry of this solid in benzene (30 mL, 0 °C) and **3b** (1.063 g, 2.65 mmol) in benzene (10 mL, 0 °C) resulted in red-brown crystals of **5b**·1/2C$_6$H$_6$ (1.076 g, 69%) after crystallization from benzene. ^{1}H NMR (500 MHz, C$_6$D$_6$, 298 K): δ 0.21 (s, 6H, SiMe$_2$), 0.47 (s, 18H, 2 SiMe$_3$), 2.16 (s, 6H, NMe$_2$), 3.69 (br s, 2H, *o*-H), 4.18 (br s, 2H, *o*-H), 4.74 (br s, 6H, *m*-H, *p*-H). ^{13}C NMR: δ 3.1 (SiMe$_2$), 7.3 (SiMe$_3$), 12.4 (GaCSi$_3$) 41.8 (NMe$_2$), 56.6 (br, *ipso*-C), 78.0 (*p*-C), 78.4 (br, *o*-C) 82.4 (br, *m*-C). MS (70 eV): m/z (%) 535 (42) [C$_{23}$H$_{40}$CrGaNSi$_3$]$^+$, 406 (27) [C$_{17}$H$_{35}$GaNSi$_3$]$^+$, 290 (22), 230 (61) [C$_9$H$_{24}$NSi$_3$]$^+$, 187 (52) [C$_7$H$_{19}$Si$_3$]$^+$, 175 (32), 129 (41) [C$_5$H$_{13}$Si$_2$]$^+$, 73 (100) [C$_3$H$_9$Si]$^+$. Anal. Calcd for C$_{26}$H$_{43}$CrGaNSi$_3$ (575.605): C, 54.25; H, 7.53; N, 2.43. Found: C, 54.05; H, 8.07; N, 2.28.

Al[1]VAP (6a). As described for **5a**, *n*BuLi (2.8 mL, 2.6 M in hexanes, 7.3 mmol), [V(C$_6$H$_6$)$_2$] (0.6019 g, 2.905 mmol), TMEDA (1.127 g, 9.70 mmol), and cyclohexane (25 mL) resulted in a solid (0.797 g, 2.38 mmol).[20] A slurry of this solid in diethyl ether (30 mL, −20 °C) and **3a** (0.863 g, 2.41 mmol) in diethyl ether (10 mL, −20 °C) resulted in dark red crystals of **6a**·1/2C$_6$H$_6$ (0.678 g, 54%) after crystallization from benzene. IR (KBr; selected value are given): 846 (s), 1012 (w), 1251 (m), 2898 (w), 2953 (w). MS (70 eV): m/z (%) 492 (100) [C$_{23}$H$_{40}$CrGaNSi$_3$]$^+$, 449 (26) [C$_{21}$H$_{35}$AlSi$_3$V]$^+$, 364 (39) [C$_{17}$H$_{35}$AlNSi$_3$]$^+$, 302 (26) [C$_{12}$H$_{33}$AlNSi$_3$]$^+$, 246 (34), 230 (26) [C$_9$H$_{24}$NSi$_3$]$^+$, 219 (40), 217 (17) [C$_8$H$_{24}$AlNSi$_2$]$^+$, 207 (11) [C$_{12}$H$_{12}$V]$^+$, 203 (21), 129 (24) [C$_4$H$_{12}$AlNSi]$^+$, 102 (19) [C$_4$H$_{12}$NSi]$^+$, 78 (52) [C$_6$H$_6$]$^+$, 73 (40) [C$_3$H$_9$Si]$^+$. Anal. Calcd for C$_{23}$H$_{40}$AlNSi$_3$V (531.812): C, 58.72; H, 8.15; N, 2.63. Found: C, 58.73; H, 8.60; N, 2.43.

---

(41) Al-Juaid, S. S.; Eaborn, C.; Hitchcock, P. B.; Hill, M. S.; Smith, J. D. *Organometallics* **2000**, *19*, 3224−3231.

(42) Steinborn, D.; Becke, F.; Boese, R. *Inorg. Chem.* **1995**, *34*, 2625−2628.

Ga[1]VAP (6b). As described for **5a**, *n*BuLi (3.0 mL, 2.6 M in hexanes, 7.8 mmol), [V(C_6H_6)$_2$] (0.6508 g, 3.141 mmol), TMEDA (1.362 g, 11.7 mmol), and cyclohexane (25 mL) resulted in a solid (0.839 g, 2.50 mmol).[20] A slurry of this solid in diethyl ether (30 mL, −20 °C) and **3b** (1.011 g, 2.51 mmol) in diethyl ether (10 mL, −20 °C) resulted in dark red crystals of **6b**·1/2C_6H_6 (0.830 g, 58%) after crystallization from benzene. IR (KBr; selected value are given): 676 (w) 845 (s), 997 (w), 1249 (m), 1458 (w), 2896 (w), 2953 (w). MS (70 eV): *m*/*z* (%) 534 (80) [$C_{23}H_{40}GaNSi_3V$]$^+$, 390 (25) [$C_{16}H_{31}GaNSi_3$]$^+$, 344 (25), 247 (21), 230 (14) [$C_9H_{24}NSi_3$]$^+$ 102 (13) [$C_4H_{12}NSi$]$^+$, 78 (100) [C_6H_6]$^+$, 73 (21) [C_3H_9Si]$^+$, 59 (13). Anal. Calcd for $C_{26}H_{43}GaNSi_3V$ (574.550): C, 54.35; H, 7.54; N, 2.44. Found: C, 54.82; H, 7.78; N, 2.41.

X-ray Structural Analysis for 2a, 4a, 4b, 5a, 5b, 6a, and 6b. Data was collected at −100 °C on a Nonius Kappa CCD diffractometer, using the COLLECT program.[43] Cell refinement and data reductions used the programs DENZO and SCALEPACK.[44] The program SIR97[45] was used to solve the structure, and SHELXL97[46] was used to refine the structure. ORTEP-3 for Windows[47] was used for molecular graphics, and PLATON[48] was used to prepare material for publication. H atoms were placed in calculated positions with U_{iso} constrained to be 1.2 times U_{eq} of the carrier atom for the methylene protons and 1.5 times U_{eq} of the carrier atom for methyl hydrogen atoms.

Acknowledgment. We thank the Natural Sciences and Engineering Research Council of Canada (NSERC Discovery Grant, J.M.), the Department of Chemistry, the Saskatchewan Structural Sciences Centre, and the University of Saskatchewan for their generous support. We thank the Canada Foundation for Innovation (CFI) and the government of Saskatchewan for funding of the X-ray and NMR facilities in the Saskatchewan Structural Sciences Centre. We thank Alan J. Lough (University of Toronto) for a helpful discussion about tilt angles.

Supporting Information Available: Crystallographic data for **2a**, **4a**, **4b**, **5a**, **5b**, **6a**, and **6b** in CIF file format. ORTEP plots for compounds **4b**, **5b**, and **6b**. This material is available free of charge via the Internet at http://pubs.acs.org.

OM060736Q

---

(43) **Nonius**; Nonius BV: Delft, The Netherlands, 1998.

(44) Otwinowski, Z.; Minor, W. In *Macromolecular Crystallography, Part A*; Carter, C. W., Sweet, R. M., Eds.; Academic Press: London, 1997; Vol. 276, pp 307−326.

(45) Altomare, A.; Burla, M. C.; Camalli, M.; Cascarano, G.; Giacovazzo, C.; Guagliardi, A.; Moliterni, A. G. G.; Polidori, G.; Spagna, R. *J. Appl. Crystallogr.* **1999**, *32*, 115−119.

(46) Sheldrick, G. M. *SHELXL97*; University of Göttingen: Germany, 1997.

(47) Farrugia, L. J. *J. Appl. Crystallogr.* **1997**, *30*, 565.

(48) Spek, A. L. *PLATON*; University of Utrecht: The Netherlands, 2001.